Early View publication on www.interscience.wiley.com
(issue and page numbers not yet assigned;
citable using Digital Object Identifier – **DOI**)

phys. stat. sol. (b), 1–5 (2008) / **DOI** 10.1002/pssb.200743450

physica status solidi b
www.pss-b.com
basic solid state physics

Atomistic force field and electronic properties of carbazole: from monomer to macrocycle

Thorsten Vehoff, James Kirkpatrick, Kurt Kremer, and Denis Andrienko*

Max Planck Institut für Polymerforschung, Ackermannweg 10, 55128 Mainz, Germany

Received 26 October 2007, accepted 23 January 2008
Published online 28 February 2008

PACS 72.20.Ee, 72.80.Le, 82.20.Wt

* Corresponding author: e-mail denis.andrienko@mpip-mainz.mpg.de, Phone: +49 6131 379 147

An atomistic force-field is developed for carbazole monomers, oligomers, and alkyne-substituted polymers. This force-field can be used to study the morphology of stacks of carbazole macrocycles. Charge transport of macrocycles in columnar arrangement is analyzed using non-adiabatic high-temperature Marcus theory.

1 Introduction Carbazole is a cheap raw material obtained, for example, from coal-tar distillation [1]. Oligomers, polymers and small molecules containing carbazole are known to easily form relatively stable radical cations, exhibit high charge carrier mobilities and good thermal and photochemical stability [2]. Carbazole derivatives are widely used in the field of organic electronics as hole-conducting materials with a wide energy gap, e.g. carbazole-based polymers were used to build dye solar cells [3]; carbazole-based small molecules were employed in blue organic light emitting diodes [4]. In addition, a π-conjugated carbazole macrocycle has recently been synthesized, which self-assembles into columnar structures [5].

To evaluate the usefulness of self-assembled structures for potential applications as well as to predict the properties of the corresponding mesophases prior to actual synthesis, one needs to accurately describe their morphologies. It has been shown that, in some cases, molecular dynamics combined with coarse-graining methods are able to describe correct morphologies [6–10]. However, current molecular dynamics force fields do not contain all parameters necessary to develop coarse-grained models of conjugated polymers, in particular polycarbazole.

In this work we first use *ab initio* methods to refine the parameters of the OPLS force field for a carbazole monomer, dimer, and oligomers with attached alkyne chains. Using this force-field, columnar phases of carbazole macrocycles can be studied. We then discuss how the obtained morphologies can be used to estimate charge mobility in a macrocycle column, with the help of thermally activated non-adiabatic Marcus' theory for charge hopping.

2 Force field parameters As a starting point, we took the OPLS force field parameters for indole [11], which is shown in Fig. 1. For alkyne side chains the OPLS united atom description was used, similar to our previous work [12, 13]. In total eight atom types were defined: the nitrogen (N_A), the carbons linking to it (C_A), the remaining carbons in the central five ring (C_B), the benzene ring carbons with hydrogens attached (C_A), the corresponding hydrogen (H_A) and the CH_2 and CH_3 united atoms of the side chain. In carbazole polymers, the carbons linking two monomers are also assigned a unique type (C_C). The atom types are illustrated in Fig. 1.

To describe polycarbazole and polycarbazole with alkyne side chains, four sets of parameters are missing in the OPLS (and most standard) force fields: those of the dihedral/improper between the carbazole and the side chain (C_N–N_A–CH_2–CH_2), and the dihedral/improper between two repeat units in a polymer (C_A–C_C–C_C–C_A). To obtain the parameters for dihedrals and impropers we first scanned the corresponding angle, optimizing the molecular geometry for each angular value using density functional theory (DFT) methods (B3LYP, 6-311g(d,p) basis set). The scan provides a set of optimized molecular structures

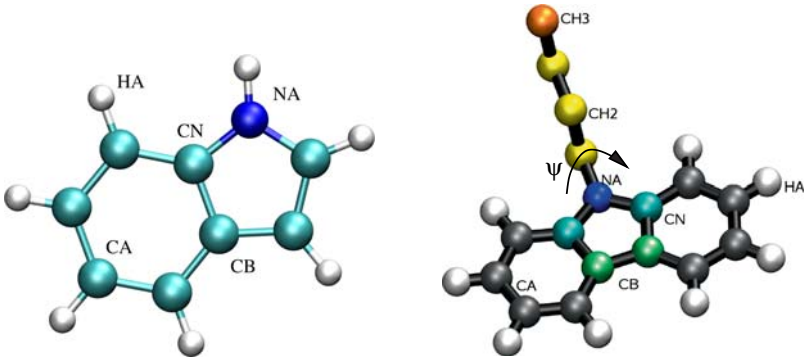

Figure 1 (online colour at: www.pss-b.com) Left: indole, from which most force field parameters were taken. Right: carbazole monomer with an attached alkyne side chain and atom types used in the force field.

and dihedral energies for each value of the dihedral angle. The second step is to evaluate the potential energy of each optimized structure using the known force field parameters with the dihedral/improper in question switched off. During the force-field-based energy evaluation the structures were further optimized with the force-field parameters while the dihedral/improper of interest is constrained. The difference between DFT and force-field-based energies is then fitted yielding the parameterization constants of the dihedral [14, 15].

The partial charges were computed by fitting to the electrostatic potential obtained from DFT calculations using the CHELPG method [16]. For the charges on a carbazole repeat unit we used the optimized structure of a carbazole pentamer. All DFT calculations were done using the GAUSSIAN package [17], all force-field computations using the GROMACS package [18]. The 1–4 interactions were scaled by a factor of 0.5 for both Lennard–Jones and Coulomb interactions in accordance with the OPLS-AA force field. For dihedral potentials the Ryckaert–Belleman function was used:

$$V_{\mathrm{RB}}(\psi) = \sum_{n=0}^{5} V_n \cos^n \psi \,. \qquad (1)$$

The DFT and force-field based energies for the side-chain dihedral are shown in Fig. 2. The dihedral scan showed that the torsional potential has a minimum at 90° when the second bond (CH_2–CH_2) is perpendicular to the core. When evaluating the force-field energies, the long range (1–4 and 1–5) interactions between carbons within the same ring were excluded, since the interaction between them is quantum mechanical and cannot be approximated by simple analytical terms. The interactions between the second side chain atom and the two closest core hydrogens were also excluded, because at closest approach the classical description is no longer valid and yields too high values in energy.

The DFT energies for a dihedral centered around the bond connecting two repeat units is shown in Fig. 3. Two different minima were found, one at approx. 45°, the other at approx. 135°. The minimum at 135° is slightly deeper, with the two nitrogens pointing in opposite directions resulting in a straight chain. For the dimer, interactions between the four closest hydrogens near the linking bond were excluded since the interaction between them leads to very strong repulsion.

The resulting force field parameters, V_n, for both dihedrals are given in Table 1.

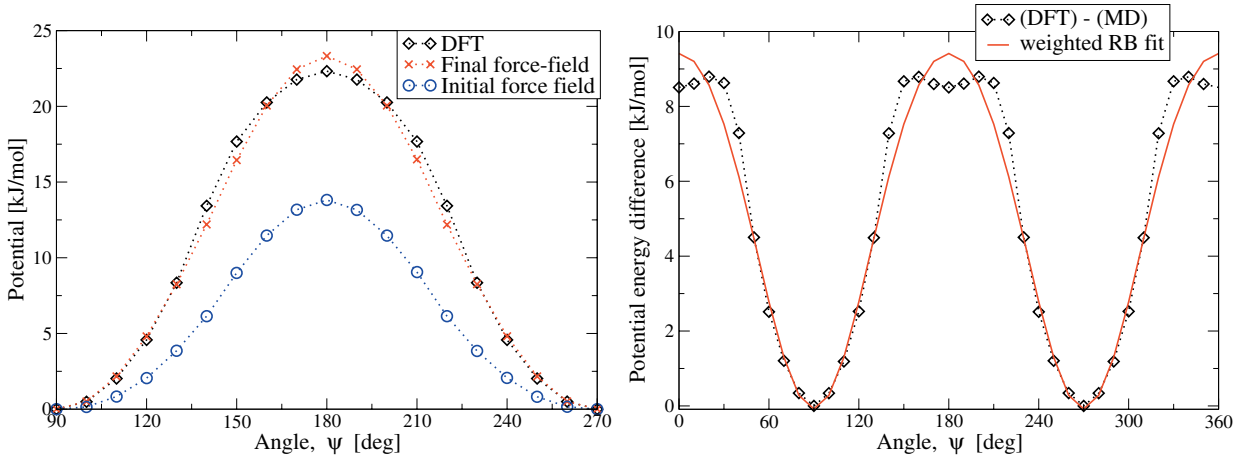

Figure 2 (online colour at: www.pss-b.com) Left: DFT (B3LYP/6-311g(d,p)) and force-field based potential energies of the C_N–N_A–CH_2–CH_2 dihedral. The initial force field refers to the OPLS energy calculation with the dihedral potential set to zero. Right: Ryckaert–Belleman fit with Boltzmann weighting exp ($-E/k_BT$) at 300 Kelvin to the difference between ab-initio and force-field-based energies.

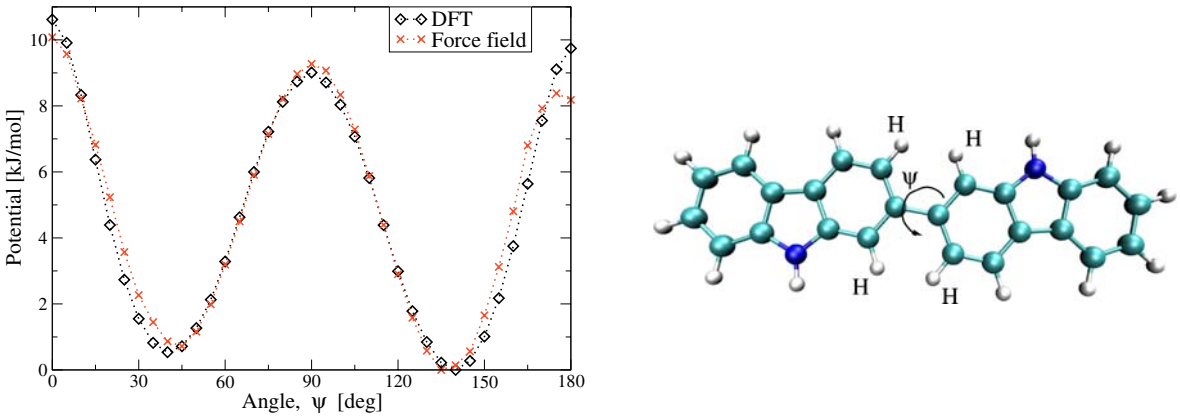

Figure 3 (online colour at: www.pss-b.com) Potential energy as function of the $C_A-C_C-C_C-C_A$ dihedral (see the left inset) angle from DFT using B3LYP/6-311(d,p) and force field with final parameters. Excluded hydrogens are labelled with H.

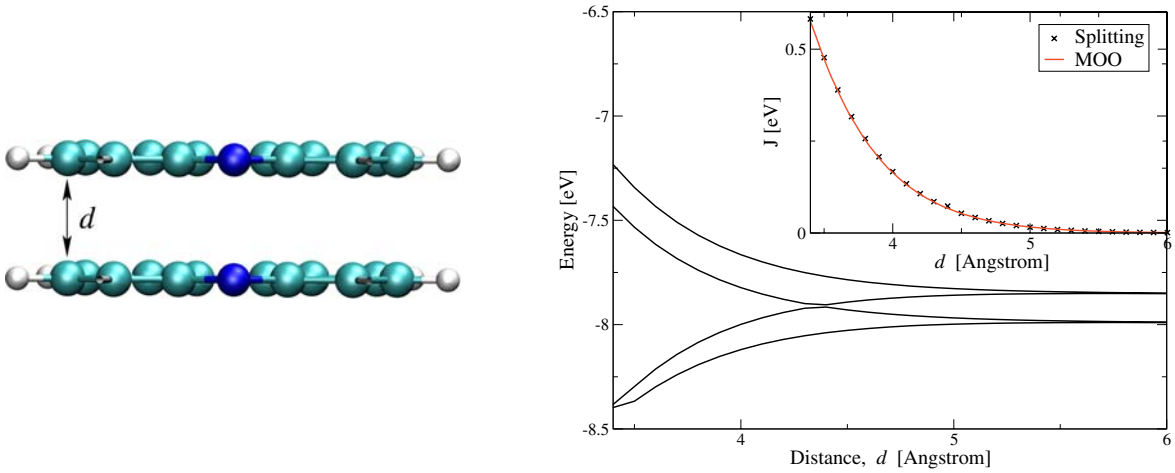

Figure 4 (online colour at: www.pss-b.com) Splitting of the HOMO energy level as a function of separation between two carbazole monomers. The inset shows the results of the molecular overlap method. Fitting to a simple exponential decay $\exp(-\alpha d)$ yields $\alpha \approx 1.76$ Å^{-1}.

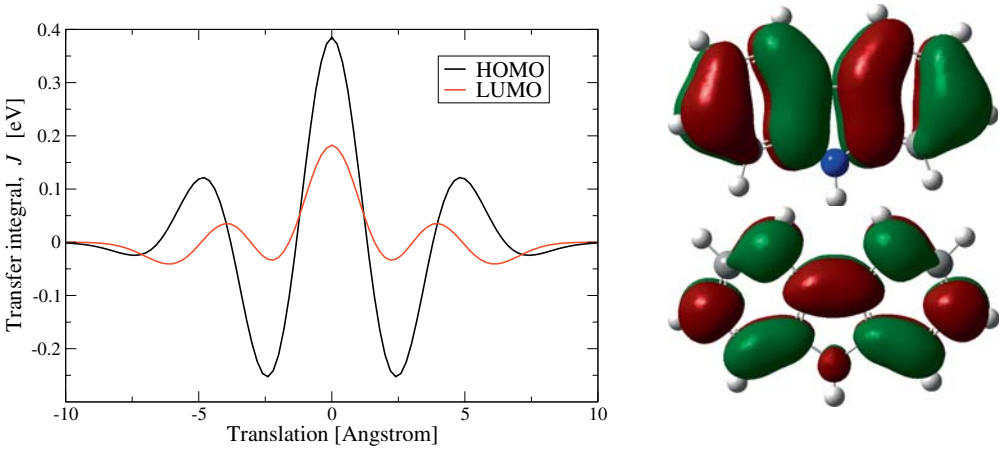

Figure 5 (online colour at: www.pss-b.com) Left: Value of overlap integral for HOMO and LUMO upon translating two carbazole monomers with respect to each other. Right: Shape of HOMO (top) and LUMO (bottom) orbitals. The distance separation is fixed at 3.6 Å.

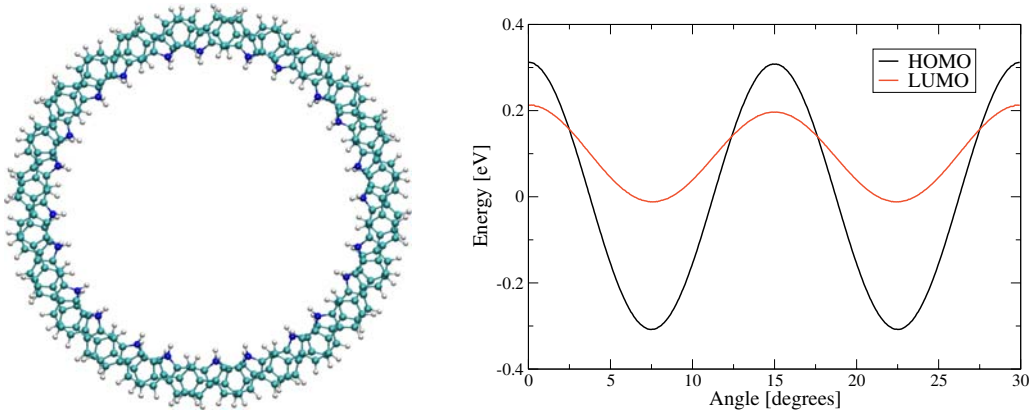

Figure 6 (online colour at: www.pss-b.com) Left: Two flat carbazole macrocycles without side chains rotated by twelve degrees with respect to each other. Right: Value of overlap integral for HOMO and LUMO upon rotating two planar carbazole macrocycles without side chains with respect to each other. The distance between the molecules is 3.6 Å.

3 Charge transport To study the charge transport we used the non-adiabatic charge transport theory as given by Marcus' theorem [19, 20], which provides the rates for charge hopping

$$\omega_{ij} = \frac{4\pi^2}{h} \frac{J_{ij}^2}{(4\pi\lambda\, k_B T)^{1/2}} \exp\left[-\frac{(\Delta G - \lambda)^2}{4\lambda\, k_B T}\right]. \quad (2)$$

Here λ is the reorganization energy, J_{ij} is the intermolecular transfer integral, h is Planck's constant, k_B the Boltzmann constant and T the temperature. For a charge transfer from molecule A to B, the internal reorganization energy is the difference in conformational energy between the initial state, where molecule A is charged and B is neutral, and the final state, where A is neutral and B charged. We ignored the external contribution to the reorganization energy. The transfer integral is the overlap of the HOMO or LUMO orbitals for hole or electron transport, respectively. To obtain the molecular orbitals required to calculate the overlap integral, we use the molecular orbital overlap (MOO) method [21, 22]. We have also checked our results by calculating the splitting of the HOMO and LUMO values for a monomer in a cofacial geometry.

The splitting of the HOMO orbital upon approach of two carbazole monomers is shown in Fig. 4. The inset shows half of the splitting versus separation as well as the results for the transfer integral obtained using the molecular orbital overlap [22] method. Note that the splitting of the HOMO level is twice the transfer integral for holes [23, 24].

Next, we calculated the overlap integral for the HOMO and the LUMO levels for the same two monomers translated with respect to each other using the molecular orbital overlap method [25]. As can be seen in Fig. 5 the overlap of the HOMO orbitals is noticeably stronger for practically all shifts, showing that carbazole is indeed a hole conducting material.

Finally, the charge transport properties of carbazole macrocycles [5] were analyzed. The optimized structure of the carbazole macrocycle without side chains was obtained starting from a flat configuration using B3LYP/3-21g(d). This is a simplification since, as was shown for the dimer, the dihedral in between repeat units is not in equilibrium at zero degrees so the units in the ring should be twisted with respect to each other. The transfer integral for two rings rotated up to thirty degrees with respect to each other was again calculated using molecular orbital overlap. This gives all relevant information, because the ring is composed of twelve repeat units. The results are shown in Fig. 6. Again, it is clear that the columnar structure of carbazole macrocycles will favor the transport of holes.

Table 1 Coefficients of the Ryckaert–Belleman function (Eq. (1)) for the side chain and dimer dihedrals.

dihedral	V_1	V_2	V_3	V_4	V_5
C_N–N_A–CH_2–CH_2	0.0	12.09	0.0	−2.60	0.0
C_A–C_C–C_C–C_A	−0.21	−34.02	−3.24	14.72	2.95

4 Conclusions & outlook At this point, we have calculated all the necessary force field parameters to run successful all atom molecular dynamics simulations of carbazole monomers with alkyne side chains, oligomers and macrocycles. We have also calculated the overlap integral for carbazole monomers, which showed that it is indeed a hole-conducting material, and checked that the molecular orbital overlap method and calculations based on the splitting of HOMO level of a dimer give the same results. Using the obtained transfer integrals the rates for the charge hopping can be calculated from Marcus' theory and the charge dynamics can be studied by solving the master equation

$$\frac{\partial P_i}{\partial t} = \sum_j [\omega_{ij} P_j (1 - P_i) - \omega_{ji} P_i (1 - P_j)]. \quad (3)$$

where the lattice points i are provided by MD simulations (centers of mass of conjugated units). The charge mobility

is then obtained by solving the stationary part of Eq. (3) and averaging the mobilities over all MD snapshots. This approach has already been tested on columnar phases of hexabenzocoronene derivatives [12, 13].

The work in progress is the validation of the force field parameters by simulating thermodynamic properties of carbazole-based organic crystals and macrocycles as well as calculation of the charge carrier mobility of columnar phases of carbazole macrocycles.

Acknowledgements This work was partially supported by DFG via grant AN 680/1-1 and via International Research Training Group between Germany and Korea.

References

[1] G. Sugerman, US Patent 3,624,174 (1971).
[2] J. V. Grazulevicius, P. Strohriegel, J. Pielichowski, and K. Pielichowski, Prog. Polym. Sci. **28**, 1297 (2003).
[3] J. Wagner, J. Piechlichowski, and A. Hinsch et al., Synth. Mater. **146**, 159 (2004).
[4] J. Lee, H. Woo, T. Meyer, and J. Park, Opt. Mater. **21**, 225–229 (2002).
[5] S.-H. Jung, W. Pisula, A. Rouhanipour, H. J. Räder, J. Jacob, and K. Müllen, Angew. Chem., Int. Ed. **45**(1), 4685–4690 (2006).
[6] F. Müller-Plathe, Chem. Phys. Chem. **3**, 754 (2002).
[7] C. F. Abrams and K. Kremer, **36**, 260 (2003).
[8] D. Reith, M. Pütz, and F. Müller-Plathe, J. Comput. Chem. **24**, 1624 (2003).
[9] S. Izvekov and G. A. Voth, J. Chem. Phys. **123**, 134105 (2005).
[10] W. Tschöp, K. Kremer, O. Hahn, J. Batoulis, and T. Bürger, Acta Polym. **49**, 75 (1998).
[11] W. L. Jorgensen, in: Encyclopedia of Computational Chemistry, Vol. 3, edited by P. v. R. Schleyer (John Wiley and Sons, New York, 1998), p. 1986.
[12] D. Andrienko, V. Marcon, and K. Kremer, J. Chem. Phys. **125**, 124902 (2006).
[13] J. Kirkpatrick, V. Marcon, J. Nelson, K. Kremer, and D. Andrienko, Phys. Rev. Lett. **98**, 227402 (2007).
[14] W. L. Jorgensen, D. S. Maxwell, and J. Tirado-Rives, J. Am. Chem. Soc. **118**, 11225–11236 (1996).
[15] A. D. Mackerell, J. Comput. Chem. **25**, 13 (2004).
[16] C. M. Breneman and K. B. Wiberg, J. Comput. Chem. **11**, 361 (1990).
[17] M. J. Frisch, G. W. Trucks, H. B. Schlegel et al., Gaussian 03, Revision C.02 (Gaussian Inc., Wallingford, CT, 2004).
[18] D. Van Der Spoel, E. Lindahl, B. Hess, G. Groenhof, A. E. Mark, and H. J. Berendsen, J. Comput. Chem. **26**(16), 1701–1718 (2005).
[19] K. F. Freed and J. Jornter, J. Chem. Phys. **51**(12), 6272–6291 (1970).
[20] R. A. Marcus, Rev. Mod. Phys. **65**, 599 (1993).
[21] M. C. Zerner, G. H. Lowe, R. F. Kirchner, and U. T. Müller-Westerhoff, J. Am. Chem. Soc. **102**, 589 (1980).
[22] J. Kirkpatrick, V. Marcon, J. Nelson, K. Kremer, and D. Andrienko, Phys. Rev. Lett. **98**, 227402 (2007).
[23] J. L. Bredas, D. Beljonne, V. Coropceanu, and J. Cornil, Chem. Rev. **104**, 4971 (2004).
[24] J. L. Bredas, J. P. Calbert, D. A. da Silva Filho, and J. Cornil, Proc. Natl. Acad. Sci. USA **99**, 5804 (2002).
[25] J. Kirkpatrick, Int. J. Quantum Chem., accepted (2007).